Movie of the structural changes during a catalytic cycle of nucleoside monophosphate kinases

Clemens Vonrhein, Gerd J Schlauderer and Georg E Schulz*

Institut für Organische Chemie und Biochemie, Albert-Ludwigs-Universität, Albertstr 21, D-79104 Freiburg im Breisgau, Germany

Background: There are 17 crystal structures of nucleoside monophosphate kinases known. As expected for kinases, they show large conformational changes upon binding of substrates. These are concentrated in two chain segments, or domains, of 30 and 38 residues that are involved in binding of the substrates N_1TP and N_2MP (nucleoside tri- and monophosphates with bases N_1 and N_2), respectively.

Results: After aligning the 17 structures on the main parts of their polypeptide chains, two domains in various conformational states were revealed. These states were caused by bound substrate (or analogues) and by crystal-packing forces, and ranged between a 'closed' conformation and a less well defined 'open' conformation. The structures were visually sorted yielding an approximately evenly spaced series of domain states that outlines the closing motions when the substrates bind. The packing forces in the crystals are weak, leaving the natural domain trajectories essentially intact. Packing is necessary, however, to produce stable intermediates. The ordered experimental structures were then recorded as still pictures of a movie and animated to represent the motions of the molecule during a catalytic cycle. The motions were smoothed out by adding interpolated structures to the observed ones. The resulting movies are available through the World Wide Web (http://bio5.chemie.uni-freiburg.de/ak movie.html).

Conclusions: Given the proliferating number of homologous proteins known to exist in different conformational states, it is becoming possible to outline the motions of chain segments and combine them into a movie, which can then represent protein action much more effectively than static pictures alone are able to do.

Structure 15 May 1995, **3**:483–490

Key words: adenylate kinase, domain movements, induced fit, X-ray structure

Introduction

X-ray diffraction analyses yield accurate static structures of crystalline proteins. Moreover, mobilities described by temperature factors (B-factors) can be assigned to each atom at resolutions better than about 2.5 Å. These B-factors indicate mobile chain segments, but cannot outline the exact motions during protein action. Attempts have been made to follow such motions in the crystal by fast Laue diffraction analyses [1]. Most substantial chain displacements, however, affect packing contacts, either prohibiting analysis by destroying the crystals, or changing the crystal form. New crystal forms have to 'settle down' before analysis [2], so that the new structure becomes just another static one.

With the advent of recombinant proteins, the number of elucidated protein structures has greatly increased. Among them are more and more homologous structures that can be related to each other. Very often, homologous structures have different ligands and/or occur in different crystal packing environments, giving rise to conformational variations. A group with particularly large conformational changes is the nucleoside monophosphate (NMP) kinase family [3]. NMP kinases catalyze the reaction

$$N_1TP{\cdot}Mg^{2+}+N_2MP \rightleftarrows N_1DP+Mg^{2+}+N_2DP$$

where N_1 and N_2 stand for nucleotide bases. Here, we relate these structures to each other, work out the conformational changes, sort the static pictures along trajectories and combine them into a movie. The presented movie shows the motions during a catalytic cycle, which lasts about 1–3 ms in this enzyme family [4,5].

Results and discussion

Alignment and superposition

An overview of 17 known NMP kinase structures is given in Table 1. Only nine of them were used, because the others either resemble the chosen representatives too closely (AK_{eco} and AK_{yst} in complex with both substrates or analogues; see Table 1 for abbreviations), or are too distantly related (GK_{yst}), or have been solved at too low a resolution (AK_{carp}). The nine selected structures were well defined (resolution range 1.63–2.6 Å) and are depicted in Figure 1.

Firstly, the selected structures had to be aligned. This was done manually according to structural superpositions (see below). Insertions/deletions were established by pin-pointing the residues that deviated most from the other superimposed chains. The result (Fig. 2) shows a consensus sequence of 206 residues for the large variants (see Fig. 2 legend for explanation) of the family. The consensus part defines the numbering. The short variants of the family ($AK1_{pig}$ and UK_{yst}; see Table 1 for abbreviations) have a 27-residue deletion around position 140.

*Corresponding author.

Table 1. Established NMP kinase structures.

No.*	Enzyme†	Ligands‡	Resolution (Å)	Reference
1	AK_{eco}	Ap_5A	1.9	[19]
–	AK_{eco}	AMPPNP, AMP	2.0	[20]
–	AK_{eco} (G10V)	Ap_5A	2.4	[21]
–	AK_{eco} (P9L)	Ap_5A	3.4	[21]
2	AK_{eco}	–	2.2	(a)
3	$AK1_{pig}$	2 SO_4^{2-}	2.1	[22]
–	$AK1_{carp}$	2 SO_4^{2-}	6.0	[23]
4	$AK2_{bov}$	SO_4^{2-}	1.92	(b)
5	$AK3_{bov}$	AMP, SO_4^{2-}	1.85	[24]
6	$AK3_{bov}$	AMP, SO_4^{2-}	2.6	(c)
7	AK_{yst}	Ap_5A, imidazole	1.63	[25]
–	AK_{yst}	Ap_5A, Mg^{2+}	1.96	[25]
–	AK_{yst} (I213F)	Ap_5A, imidazole	2.2	(d)
8	AK_{yst} (D89V,R165I)	$AMPPCF_2P$	2.4	(b)
9	UK_{yst}	2 ADP	2.1	[26]
–	UK_{yst}	ADP, AMP	1.9	[27]
–	GK_{yst}	GMP, SO_4^{2-}	2.0	[28]

*Only the numbered structures are used in this study. †Source of enzyme: AK_{eco}, adenylate kinase from *E. coli*; $AK1_{pig}$, cytosolic adenylate kinase from muscle; $AK1_{carp}$, cytosolic adenylate kinase from carp muscle; $AK2_{bov}$, adenylate kinase from beef liver mitochondria (intermembrane space); AK_{yst}, adenylate kinase from yeast; UK_{yst}, uridylate kinase from yeast; GK_{yst}, guanylate kinase from yeast. ‡Ap_5A is diadenosine pentaphosphate, AMPPNP and $AMPPCF_2P$ (gift from G Blackburn) are non-hydrolyzable analogues of ATP. Unpublished data from: (a), G Schlauderer, CW Müller, J Reinstein & GE Schulz; (b), G Schlauderer & GE Schulz; (c), C Vonrhein & GE Schulz (the space group is different from the one for structure 5); (d), P Spürgin, U Abele & GE Schulz.

The large conformational changes in the NMP kinase family were recognized earlier [3]. They have been described [3,6] as motions of internal chain segments relative to the main body containing the central parallel β-sheet (Fig. 1). The major moving segments are termed the NMP_{bind} domain (residues 30–59) and the LID domain (residues 120–157); the remaining parts constitute the CORE domain (residues 1–29, 60–119, 158–206). To elaborate the motions of the NMP_{bind} and LID domains, we superimposed all structures on their CORE domains. The closed down structure of AK_{eco}:Ap_5A (number 1 of the nine structures used, see Table 1) was taken as a reference, and all other structures were transformed by the rotation/translation movement that best fitted the CORE domain of structure 1. The superposition data are given in Table 2.

By using a rather small (1 Å) cutoff in the program Overlay [7], the CORE superpositions were tightened to the highly conserved central β-sheet. The residual root mean square (rms) Cα differences (ΔCα) in the CORE domain are smallest for structures 7 and 9, which contain both substrates (Ap_5A or two ADP molecules, respectively) like the reference structure 1, and are larger for the other structures. This indicates some change in the CORE domain on substrate binding as reported previously for one of the cases [6]. CORE domain differences resulting from evolutionary changes are unlikely, as there is no correlation between the rms ΔCα values and the percentage of identical residues (Table 2).

Trajectories

After aligning all structures with the CORE domain of structure 1, we visualized the resulting conformations of the NMP_{bind} and LID domains on a graphics display. We then established the order of the structures, with respect to NMP_{bind}, defining a trajectory for this domain. The structure series runs from *a* to *i*, recording a motion from an open to a closed conformation (Table 2). Note that the reference structure 1 is not one of the endpoints of this trajectory. The manual ordering is confirmed by the maximum Cα displacements, and it approximately follows the polar rotation angles of the domain.

The corresponding order of the LID domains was again established manually and runs from *A* to *G*, recording a motion from an open to a closed conformation (Table 2). This order is confirmed by the maximum Cα displacements and also by the polar rotation angles of the domain. The residual ΔCα values for the LID domain are about half those of the NMP_{bind} domain, although the LID domain is 1.3× larger, demonstrating that the LID domain moves much more like a solid block than the NMP_{bind} domain. As the orderings for NMP_{bind} and LID are different, these domains move independently from each other, in agreement with the observed random-bi-bi kinetics (i.e. the random order of substrate binding) [8].

Animation

The two resulting picture series of domain positions were turned into movies by displaying the pictures with time intervals of ~1 s on a computer screen. These movies were rather jerky, but represented purely experimental data. To smooth out the motions, we used the experimental structures as safe-points and calculated a number of interpolated structures in between them (Table 3). The numbers of interpolated structures ranged from 8 for the smallest to 27 for the largest structural changes, along the series. The interpolation was performed locally using a window of nine residues sliding over the whole chain (see below). This also ensured smoothness for motions of segments that deviated strongly from the common best rotation/translation of the respective domain.

The resulting movies contained 136 structures for NMP_{bind} and 90 for LID. They are available through the World Wide Web (WWW) [9] or file transfer protocol (FTP; see below). From each movie we selected 40 structures, approximately equally spaced along the trajectory, and present them in Figures 3 and 4 for the NMP_{bind} and LID domain motions, respectively. These figures can be used to produce flicker books (see legends for instructions).

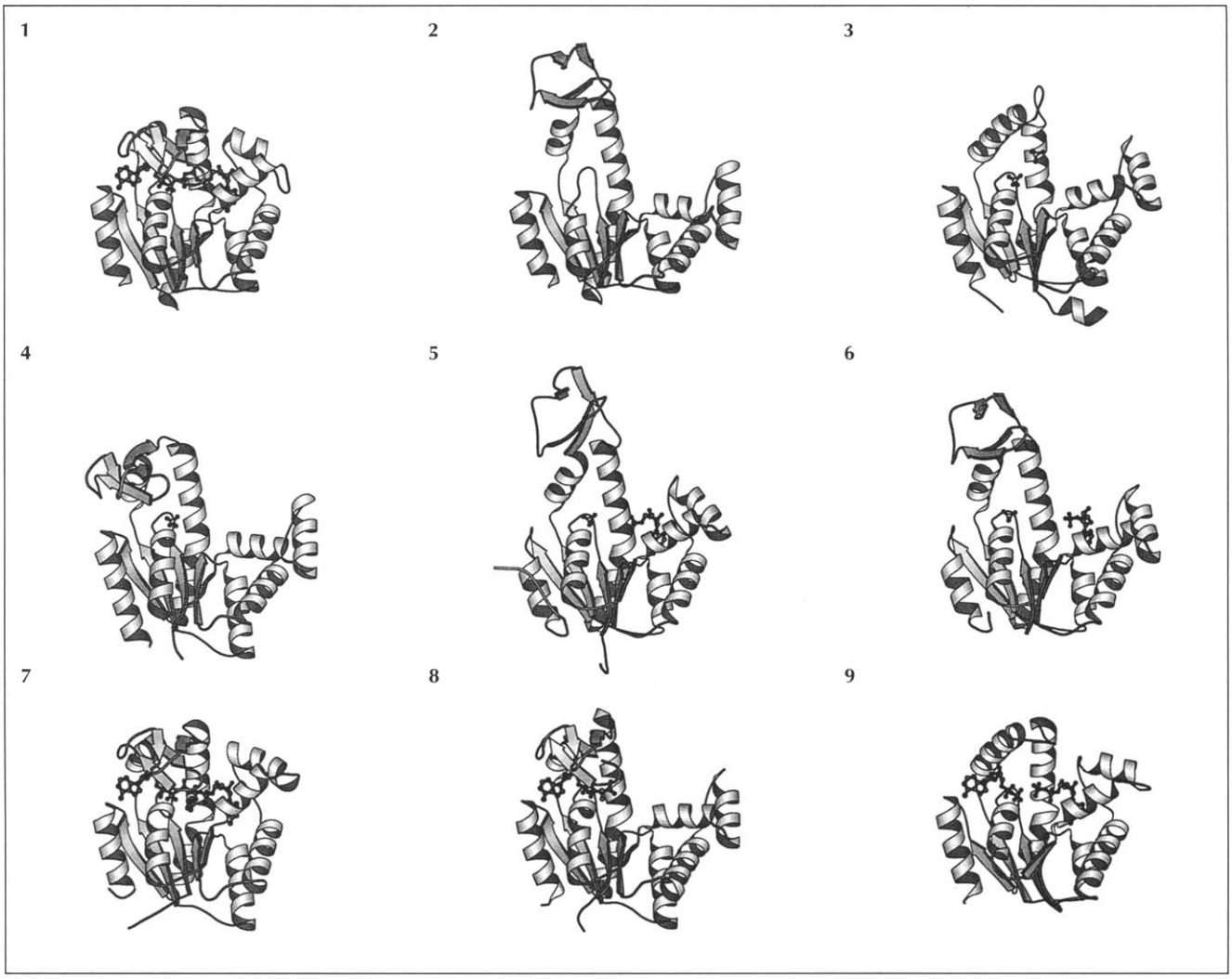

Fig. 1. Ribbon representation of all established structures used in the movie, including the ligands, which are shown as ball and stick models. 1, AK_{eco}:Ap_5A; 2, AK_{eco}; 3, AK1; 4, AK2; 5, AK3:AMP; 6, AK3:AMP; 7, AK_{yst}:Ap_5A; 8, AK_{yst}:AMPPCF$_2$P; 9, UK_{yst}:ADP:ADP. For details see Table 1.

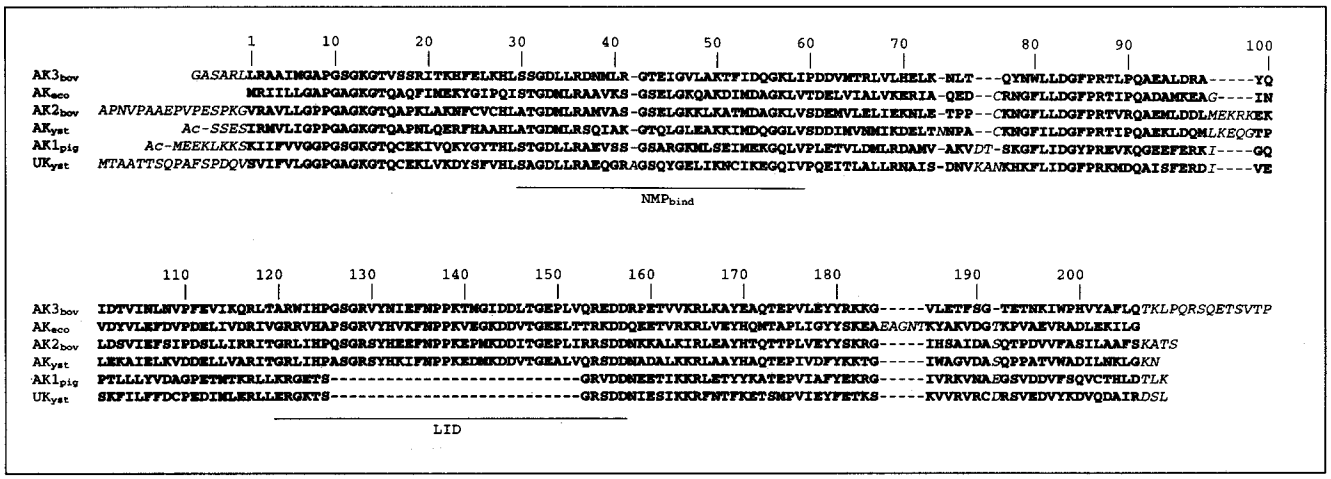

Fig. 2. Sequence alignment of the reported NMP kinases as based on the spatial structures (see text). Residues that are common between kinases are emphasized by bold type. This is the consensus set of 206 residues and it forms the basis for the numbering scheme. The domains NMP_{bind} and LID are defined according to an earlier comparison [3]. The first four structures are called large variants of the family because they contain the full LID domain. The last two structures are small variants as they have a large (27 residue) deletion in the LID domain.

Table 2. Structural superpositions on the CORE domain showing the motions of NMP_{bind} and LID.

		CORE			NMP_{bind}				LID			
No.	Crystal structure	Residue identities† (%)	Number of superimposed Cα atoms‡	Rms ΔCα§ (Å)	Visual order#	Max. ΔCα** (Å)	Rotation angle†† (°)	Rms ΔCα†† (Å)	Visual order#	Max. ΔCα** (Å)	Rotation angle†† (°)	Rms ΔCα†† (Å)
1	$AK_{eco}:Ap_5A$	–	–	–	*g*	0	0	0	*G*	0	0	0
2	AK_{eco}	100	52	2.3	*a*	18	50	1.8	*B*	24	54	0.5
3	$AK1_{pig}$	32	66	1.9	*e*	12	36	2.3	–	–	–	–
4	$AK2_{bov}$	39	49	2.2	*b*	17	51	2.5	*D*	14	33	1.7
5	$AK3_{bov}:AMP$	34	49	2.1	*f*	4	5	1.7	*A*	31	86	1.5
6	$AK3_{bov}:AMP$	34	44	2.4	*d*	12	18	2.4	*C*	22	57	1.0
7	$AK_{yst}:Ap_5A$	41	107	1.1	*h*	6	–7	1.7	*F*	5	8	0.6
8	$AK_{yst}:AMPPCF_2P$*	40	56	2.2	*c*	16	40	1.9	*E*	6	9	1.3
9	$UK_{yst}:ADP:ADP$	28	91	1.3	*i*	6	–6	2.4	–	–	–	–

*This complex was with the mutant enzyme AK_{yst} (D89V, R165I). †All 138 residues of the CORE domain were compared with those of AK_{eco} (Fig. 2). ‡Superposition performed using the program Overlay [7] with a cutoff of 1 Å, which selected the given number of Cα atoms. §The residual rms ΔCα was calculated for all 138 residues of the CORE domain. #See text. **This is the maximum displacement of a Cα atom from the moving domain with respect to the reference structure 1. ††The moving domain was compared with the respective domain in reference structure 1, and the change was described by the best rotation/translation. The polar rotation angle of this rotation is given together with the residual rms ΔCα deviation. The rotation axis changed from comparison to comparison. The rotation angle is negative if it is related to the same general direction of the polar axis.

Table 3. Structure series and interpolation for the two domains, NMP_{bind} and LID.

NMP_{bind}			LID		
Visual ordering	Exptl. structure no.	No. of interpolated structures	Visual ordering	Exptl. structure no.	No. of interpolated structures
a	2		*A*	5	
		14			13
b	4		*B*	2	
		13			11
c	8		*C*	6	
		21			27
d	6		*D*	4	
		12			9
e	3		*E*	8	
		18			15
f	5		*F*	7	
		18			8
g	1		*G*	1	
		17			
h	7				
		14			
i	9				
Total	9 +	127 = 136	Total	7 +	83 = 90

For a larger audience, we produced a videotape of the 90 picture series of the LID motion. In this videotape, the molecule is rotated by 90° around a vertical axis with respect to Figure 4, such that NMP_{bind} becomes clearly visible. However, because the large LID motion is more obvious, some unavoidable back and forth motions of NMP_{bind} are easily tolerated by the viewer. The underlying picture series used to produce the videotape, together with some computer readable files, can be obtained through WWW [9] or FTP (see below). Videotapes will be sent on request.

Conclusions

The presented movies demonstrate that protein structures have left the realm of static structures as determined in crystals by X-ray diffraction or in solution by NMR. Because of the increasing number of homologous structures with different ligands, in various crystal packings, we are now able to sort the structures along the trajectories of given regions and to display them as movies in atomic detail. Interpolation helps the eye to resolve movements without interfering with reality. Random crystal contacts perturb the motions, but can be tolerated. Just like Daguerre's static pictures from the middle of the last century learned how to 'run' by the end of that century, we expect to see more and more static proteins becoming lively actors in the future.

Fig. 3. (see facing page) Picture series 1 to 40 for the NMP_{bind} motion, representing an equally spaced selection from the 136 pictures of the movie. The LID domain has been cut away, because the series includes both small and large variants of the NMP kinase family (Fig. 2). The observed structures, *a* to *i*, are indicated. The pictures can be cut out and stapled at the left-hand side to produce a flicker book. During stapling the pictures should be kept aligned by holding them with a clamp.

Fig. 4. (see over page) Picture series 1 to 40 for the LID motion, representing an equally spaced selection from the 90 pictures of the movie. The observed structures, *A* to *G*, are indicated. The pictures can be cut out and stapled at the left-hand side to produce a flicker book, as described in the legend for Figure 3.

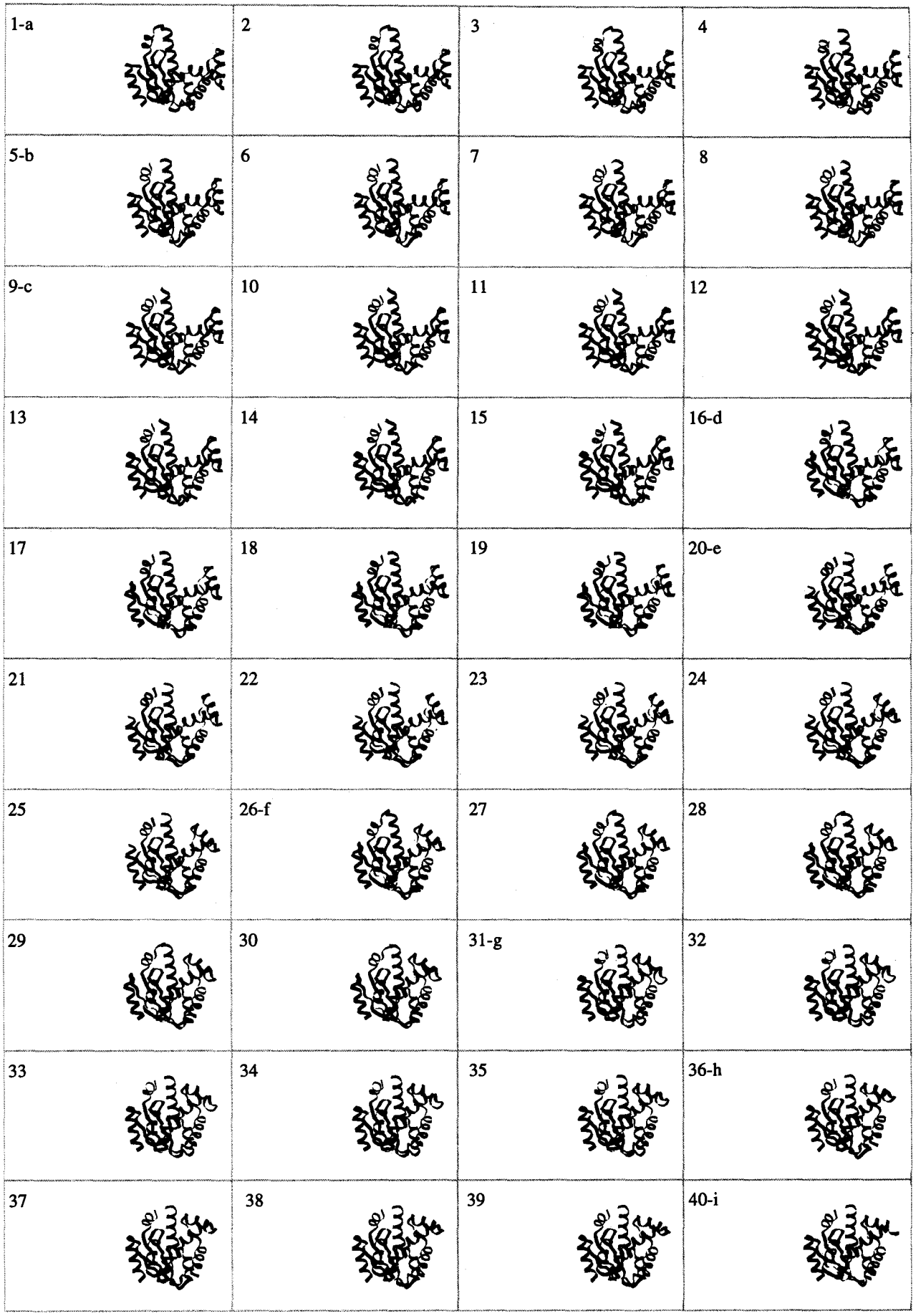
1-a
2
3
4
5-b
6
7
8
9-c
10
11
12
13
14
15
16-d
17
18
19
20-e
21
22
23
24
25
26-f
27
28
29
30
31-g
32
33
34
35
36-h
37
38
39
40-i

1-A 	2 	3 	4 
5 	6 	7 	8 
9-B 	10 	11 	12 
13-C 	14 	15 	16 
17 	18 	19 	20 
21 	22-D 	23 	24 
25 	26 	27 	28 
29 	30-E 	31 	32 
33 	34 	35 	36-F 
37 	38 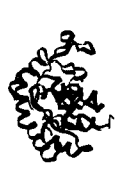	39 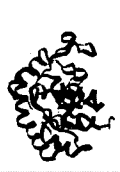	40-G 

Biological implications

For a long time, it has been proposed that kinases undergo large movements during catalysis [10], because they have to shield their active center from water in order to avoid ATP hydrolysis. In an effort to confirm the expected conformational changes, the small nucleotide monophosphate (NMP) kinases have been studied extensively [11]. The large number of solved NMP kinase structures has now confirmed these expectations. Moreover, these structures allowed us to follow the motions much more closely than before, because various intermediate states are frozen in crystals. We found that the frozen position of a domain depends on the crystal-packing forces giving rise to many more conformational states than just an 'open' and a 'closed' one, without and with bound ligand, respectively. Ordering of these intermediates with additional computational smoothing allows us to represent domain movements as a movie. Such a movie approximates the action of a protein much more accurately than a single structure is able to do; it represents a novel way of realistically visualizing our knowledge of life at the atomic level.

As isolated static structures indicating large motions are also known for other proteins [12–15], one should expect that in the near future, more and more intermediate states will be elucidated, giving rise to similar movies representing the actions of other proteins.

Materials and methods

Alignment

Structure 1 contains the LID in its most completely closed conformational state (Fig. 1) and was therefore chosen as a reference for alignment and domain motions. The chain alignment of Figure 2 began with structural superpositions of the CORE domains using the program Overlay [7] with a 1.5 Å cutoff. These superpositions concerned mainly the central β-sheets; they were followed by visual inspections of other parts of the CORE domain to establish insertions and deletions. The consensus region was limited by the *E. coli* enzyme with the shortest N and C termini. The assignment of domains NMP_{bind} and LID was taken from an earlier comparison [3]. As the small variants (structures 3 and 9) have almost no LID, they were excluded from the study of the LID motion. Apart from the difference between large and small variants in LID, there are five positions with insertions, leading to fairly small discontinuities in the structure series (Table 2), which are based on the 206 consensus residues.

Interpolation

For interpolating along the LID trajectory, we used a nine-residue peptide window sliding from the N terminus to the C terminus of the consensus sequence. For the NMP_{bind} trajectory, the LID domain was removed, and the peptide window moved between the ends of the remaining segments. For interpolating between two given, consecutive, experimental structures X and Y, we determined the best peptide rotation/translation at each window position j (position of central residue) with the program X-PLOR [16] and described it by polar axis orientation, polar rotation angle κ_j and translation $\vec{t}_j$. The number of interpolated structures, N (Table 3), was chosen such that the largest κ_j was subdivided into steps of about 2° for NMP_{bind} and 4° for LID. The interpolated structures n=1,2,...N were produced by applying the respective rotation/translation with $\kappa_j \cdot n/N$ and $\vec{t}_j \cdot n/N$ to each residue j of structure X. The first and last four residues of each chain were not altered. The applied local interpolation kept all distances between subsequent Cα atoms in an acceptable range, resulting in a smooth motion from structure X to structure Y. All structures were represented by the program Raster3D [17].

Animation

For the production of movies consisting of the 136 and 90 pictures of the NMP_{bind} and LID motions, respectively, the Raster3D files were converted with programs ImageMagick and Mpeg_Encode and viewed with Mpeg_Play. The Mpeg files and Mpeg viewer for DOS and UNIX systems are available through WWW [9] (http://bio5.chemie.uni-freiburg.de/ak_movie.html) and anonymous FTP (bio5.chemie.uni-freiburg.de:/pub/ak_movie) together with a manual.

The third movie contains only the structure series of the LID motion as drawn by the programs MOLSCRIPT [18] and Raster3D [17] in color and shading. For this purpose, a general secondary structure was assigned. This movie is more beautiful than the first two and it has been converted to a videotape (Fa. Profilm Team, Freiburg im Breisgau) to make it available for larger audiences.

Acknowledgements: We thank G Blackburn, CW Müller, K Proba, J Reinstein, E Schiltz and A Wittinghofer for contributions to the structures that have not been published yet. The project was supported by the Deutsche Forschungsgemeinschaft (SFB-60) and the Land Baden-Württemberg.

References

1. Taubes, G. (1994). X-ray movies start to capture enzyme molecules in action. *Science* **266**, 364–365.
2. Schlichting, I., *et al.*, & Goody, R.S. (1990). Time-resolved X-ray crystallographic study of the conformational change in Ha-Ras p21 protein on GTP hydrolysis. *Nature* **345**, 309–315.
3. Schulz, G.E., Müller, C.W. & Diederichs, K. (1990). Induced-fit movements in adenylate kinases. *J. Mol. Biol.* **213**, 627–630.
4. Noda, L., Schulz, G.E. & von Zabern, I. (1975). Crystalline adenylate kinase from carp muscle. *Eur. J. Biochem.* **51**, 229–235.
5. Ito, Y., Tomasselli, A.G. & Noda, L. (1980). ATP:AMP phosphotransferase from baker's yeast. *Eur. J. Biochem.* **105**, 85–92.
6. Gerstein, M., Schulz, G.E. & Chothia, C. (1993). Domain closure in adenylate kinase. Joints on either side of two helices close like neighboring fingers. *J. Mol. Biol.* **229**, 494–501.
7. Kabsch, W. (1976). A solution for the best rotation to relate two sets of vectors. *Acta Crystallogr. A* **32**, 922–922.
8. Rhoads, D.G. & Lowenstein, J.M. (1968). Initial velocity and equilibrium kinetics of myokinase. *J. Biol. Chem.* **243**, 3963–3972.
9. Schatz, B.R. & Hardin, J.B. (1994). NCSA Mosaic and the World Wide Web — global hypermedia protocols for the Internet. *Science* **265**, 895–901.
10. Jencks, W.P. (1975). Binding energy, specifity and enzymatic catalysis: the circe effect. *Adv. Enzymol.* **43**, 219–410.
11. Schulz, G.E. (1992). The induced-fit movements in adenylate kinases. *Faraday Discuss.* **93**, 85–93.
12. Bennett, W.S., Jr. & Steitz, T.A. (1980). Structure of a complex between yeast hexokinase A and glucose. Detailed comparisons of conformation and active site conformation with the native hexokinase B monomer and dimer. *J. Mol. Biol.* **140**, 211–230.
13. Dixon, M.M., Nicholson, H., Shewchuk, L., Baase, W.A. & Matthews, B.W. (1992). Structure of a hinge-bending bacteriophage

T4 lysozyme mutant, Ile3→Pro. *J. Mol. Biol.* **227**, 917–933.
14. Anderson, B.F., Baker, H.M., Norris, G.E., Rumball, S.V. & Baker, E.N. (1990). Apolactoferrin structure demonstrates ligand-induced conformational change in transferrins. *Nature* **344**, 784–787.
15. Ikura, M., Clore, G.M., Gronenborn, A.M., Zhu, G., Klee, C.B. & Bax, A. (1992). Solution structure of a calmodulin-target peptide complex by multidimensional NMR. *Science* **256**, 632–638.
16. Brünger, A.T., Kuriyan, J. & Karplus, M. (1987). Crystallographic R-factor refinement by molecular dynamics. *Science* **235**, 458–460.
17. Merritt, E.A. & Murphy, M.E.P. (1994). Raster3D version 2.0, a program for photorealistic molecular graphics. *Acta Crystallogr. D* **50**, 869–873.
18. Kraulis, P.J. (1991). MOLSCRIPT: a program to produce both detailed and schematic plots of protein structures. *J. Appl. Crystallogr.* **24**, 946–950.
19. Müller, C.W. & Schulz, G.E. (1992). Structure of the complex between adenylate kinase from *Escherichia coli* and the inhibitor Ap_5A refined at 1.9 Å resolution. *J. Mol. Biol.* **224**, 159–177.
20. Berry, M.B., Meador, B., Bilderback, T., Liang, P., Glaser, M. & Phillips, G.N., Jr. (1994). The closed conformation of a highly flexible protein: the structure of *E. coli* adenylate kinase with bound AMP and AMPPNP. *Proteins* **19**, 183–198.
21. Müller, C.W. & Schulz, G.E. (1993). Crystal structures of two mutants of adenylate kinase from *Escherichia coli* that modify the Gly-loop. *Proteins* **15**, 42–49.
22. Dreusicke, D., Karplus, P.A. & Schulz, G.E. (1988). Refined structure of porcine cytosolic adenylate kinase at 2.1 Å resolution. *J. Mol. Biol.* **199**, 359–371.
23. Reuner, C., Hable, M., Wilmanns, M., Kiefer, E., Schiltz, E. & Schulz, G.E. (1988). Amino acid sequence and three-dimensional structure of cytosolic adenylate kinase from carp muscle. *Protein Seq. Data Anal.* **1**, 335–343.
24. Diederichs, K. & Schulz, G.E. (1991). The refined structure of the complex between adenylate kinase from beef heart mitochondrial matrix and its substrate AMP at 1.85 Å resolution. *J. Mol. Biol.* **217**, 541–549.
25. Abele, U. & Schulz, G.E. (1995). High resolution structures of adenylate kinase from yeast ligated with inhibitor Ap_5A showing the pathway of phosphoryl transfer. *Protein Sci.*, in press.
26. Müller-Dieckmann, H.J. & Schulz, G.E. (1994). The structure of uridylate kinase with its substrates, showing the transition state geometry. *J. Mol. Biol.* **236**, 361–367.
27. Müller-Dieckmann, H.J. & Schulz, G.E. (1995). Substrate specificity and assembly of the catalytic center derived from two structures of ligated uridylate kinase. *J. Mol. Biol.* **246**, 522–530.
28. Stehle, T. & Schulz, G.E. (1992). Refined structure of the complex between guanylate kinase and its substrate GMP at 2.0 Å resolution. *J. Mol. Biol.* **224**, 1127–1141.

Received: **15 Feb 1995**; revisions requested: **8 Mar 1995**; revisions received: **21 Mar 1995**. Accepted: **23 Mar 1995**.